

RELIABILITY BASED DESIGN FOR DEFORMATION TARGETED SEGMENT MECHANICALLY STABILIZED EARTH WALL

Yi-Che Wu¹, Chia-Nan Liu^{2*}, and Bo-Hung Lin³

ABSTRACT

The application of probabilistic concept has been pervaded in the analysis and design of geotechnical structures recently. For example, the reliability of stability, instead of deterministic stability, for mechanically stabilized earth (MSE) walls has been popular. This paper presents a study of reliability analysis of MSE wall targeting on the wall performance, explicitly the maximum wall face deformation. First, a numerical model for simulating a segment MSE wall is developed. This numerical model is verified through a promising comparison with deformation and stress measurement as reported in the literature. A numerical experiment set consisting of 729 simulations by varying important design parameters including wall height, wall inclination, soil friction angle, stiffness of segments, extent of reinforcement, and magnitude of surcharge is then conducted. The database of maximum wall deformation under different combination of design parameters of MSE wall is regressed, using the response surface method to build an approximate equation between design parameters and dimensionless maximum wall deformation. The suitability of approximate equation is examined by its sound comparison with numerical simulation results. Types of model uncertainties in the approximate equation from numerical simulation results and from the measurement records are then estimated. A series of parametric analysis is conducted to identify how the magnitude and uncertainty in the parameters affect the probabilistic performance of wall face deformation. The procedures of how to perform probabilistic analysis of segmental MSE wall, under certain constrain of maximum wall face deformation, is provided by charts showing reliability versus design parameters.

Key words: Probabilistic analysis, regression, Monte Carlo Simulation, MSE wall, reliability based design.

1. INTRODUCTION

Geosynthetic material has been commonly applied in reinforcing soil structures, such as retaining walls. Various approaches have been proposed for reasonable design and stability analysis of reinforced earth retaining wall. Among them, limit equilibrium analysis is mostly used to assess the safety factor for failure of retaining wall, though different approaches according to different assumptions on active soil pressure and effect of geosynthetic reinforcement are applied. Similar to conventional analysis of retaining wall, the limit equilibrium methods calculate factor of safety as an index of the stability of geosynthetic reinforced retaining walls. Most geosynthetic reinforced soil structures have performed satisfactorily. Suah and Goodings (2001) conducted 27 centrifuge tests of physical model of geotextile reinforced vertical walls with backfill soils ranging from sand to clay. They found none of the models failed of geotextile pull out. Rowe and Skinner (2001) reported that the measured geosynthetic strains of an 8m high, segmented concrete face geogrid reinforced soil wall constructed on a layered foundation stratum in Japan were all below 1.5%. Bathurst *et al.* (2002) also showed that reinforcement strains in four

instrumented field walls did not exceed 1% after construction. Hirakawa *et al.* (2004) conducted laboratory model tests of reinforced soil retaining wall. The test results showed only a 0.4% strain was measured on weak polyester geogrid when the model test was loaded to 480 kPa and followed by a series of sustained and cyclic vertical loading. Hatami and Bathurst (2005) conducted numerical and physical tests of three 3.6 m high test walls reinforced by geogrid of different stiffness, spacing, and structural facing. Results showed that the strains in the reinforcement layers were typically less than 1% for the wall models at the end of construction. After reviewing a database of instrumented and monitored full-scale field and laboratory walls, Allen *et al.* (2002) and Bathurst *et al.* (2005) concluded that the existing design methods led to an excessive conservative design of geosynthetic reinforced structures required to generate satisfactory long-term wall performance. The stability performance of reinforced zone has been performed successfully because of the well-developed design requirement, widespread experiences, and most importantly, conservative design methodologies based on limit states of geosynthetics. For most of the retaining wall or embankment that is reinforced by geosynthetic, the deformation of the soil structure, rather than the stability, is more concerned. The deformation of MSE wall has drawn a lot of interest over the last decades. Most studies used field data (Onodera *et al.* 2004; Duijnen *et al.* 2014), laboratory experiments (Bathurst *et al.* 2009; Ruiken *et al.* 2010; Ehrlich *et al.* 2012), or numerical analysis (Liu *et al.* 2009; Kibria *et al.* 2010; Yang *et al.* 2012; Ehrlich and Mirmoradi 2013) to investigate the deformation of rigid-face or wrapped-face MSE wall under construction or after the end of construction. However, the design approach based on deformation is seldom provided.

Manuscript received February 18, 2019; revised July 15, 2019; accepted August 6, 2019.

¹ Ph.D. Student, Civil Engineering Department, National Chi Nan University, Taiwan 545, R.O.C.

^{2*} Professor (corresponding author), Civil Engineering Department, National Chi Nan University, Taiwan 545, R.O.C. (e-mail: cnliu@ncnu.edu.tw).

³ Postdoctoral Research Fellow, Civil Engineering Department, National Chi Nan University, Taiwan 545, R.O.C.

The deterministic properties of soil and reinforcing material are adopted in the assessment of factor of safety, though the variability in the soil and geosynthetic material is not considered in conventional limit equilibrium methods. This leads to the probabilistic analysis for stability of reinforced retaining walls. For example, Basheer and Najjar (1994) presented a reliability-based design of reinforced earth retaining walls. They applied the first-order Taylor series approximation to determine the mean and variance for the width and length of the reinforcing ties for the reinforced earth retaining walls supporting sandy soils. Basma *et al.* (2003) applied the mean value first order second moment (MVFOSM) approach to advance the existing Rankin method of lateral earth pressure by including the variation of internal friction angle and unit weight of soil in the design process. The width and length of the reinforcing material (metallic strip) are then evaluated through a predetermined reliability. Chalermyanont and Benson (2004, 2005a, 2005b) used Monte Carlo simulation to develop a probabilistic design method for internal, external, and systematic stability of MSE walls backfilled with and founded on cohesionless soil. Sayed *et al.* (2008) conducted reliability analysis of reinforced soil retaining walls using three reliability methods and concluded that the friction angle of backfill soil is the most sensitive random variable affecting the stability of the reinforced soil walls, under static and seismic conditions. In general, the reliability approach considers the possible variations in the design parameters and gives more realistic estimates of the safety of the reinforced retaining wall and the possible risk of failure.

The aim of this study is to present probabilistic analysis of geosynthetic reinforced segment wall. Recognizing the fact that few catastrophic failure cases have been occurred under the guidance of conservative design and construction standards, the serviceability of reinforced wall, instead of the factor of safety for the limit state stability, is of interest. In terms of serviceability, the maximum wall face deformation is the target in this study. The details of analysis approach includes developing numerical models, conducting numerical experiments, regressing approximated equations, performing Monte-Carlo simulations for probabilistic analysis, and how to design based on acceptable performance criterion will be presented in the following sections.

2. NUMERICAL EXPERIMENTS OF MAXIMUM FACE DEFORMATION OF SEGMENT MSE WALL

Since the maximum wall face deformation is the target in this study, limit equilibrium approaches are not as suitable to describe the wall face deformation, as well as to describe deformation behavior of the geosynthetic reinforced retaining wall. The finite difference-based program Fast Lagrangian Analysis of Continua – FLAC (Itasca 2001) was used to develop the numerical model in this study. Hatami and Bathurst (2005) presented a well-controlled laboratory model test of segmental MSE wall at Royal Military College (RMC). They also used the FLAC code to numerically model the behaviors of their model walls. In this study, a numerical model based on FLAC code was developed following the material properties and constitutive models presented in Hatami and Bathurst (2005). The analysis results indicate well agreement between numerical analysis results and the recorded wall face deformation and geosynthetic strains of the physical model walls built

at RMC. The satisfactory comparison justifies the appropriateness of the numerical model developed in this study. The detail of development and justification of the numerical model please refer to Lin *et al.* (2016).

Due to the numerical simulation of deformation behavior of geosynthetic reinforced retaining wall takes much longer running time, a preliminary parametric study was conducted to determine the variables that have significant influence. Only those variables found significant were treated as random variables in the subsequent probabilistic numerical simulation. The parameters which describe the material properties for sand backfill, and segment facing are studied. These parameters are: friction angle of backfill soil (ϕ_s), unit weight of backfill soil (γ_s), elastic modulus of backfill soil (E_s), shear stiffness between segment blocks (k_{sbb}), shear stiffness between segment block and backfill soil (k_{ssb}) and the grout stiffness ($k_{bond,sr}$) between soil and reinforcement. The preliminary parametric analysis is performed under a deterministic framework. The test value of single parameter is input into the numerical model while the value of other parameters keeps unchanged. The change percentage of simulated maximum facing deformation is normalized by the change percentage of parameter value. The analysis results are shown in Fig. 1.

Generally, the effect of parameter on the wall face deformation is nonlinear. Compared with the friction angle of backfill soil (ϕ_s), and shear stiffness between segment blocks (k_{sbb}), the elastic modulus of backfill soil and shear stiffness between segment block and backfill soil has relatively insignificant effect on the wall face deformation. The results are similar to the finding reported in Rowe and Ho (1998) that soil Young's modulus, soil-facing interface friction angle is less important to friction angle of backfill soil. Therefore, they are not included into following numerical experiments. The difference of face rigidity has been highlighted by a comparison between segmented block wall and wrapped wall (Bathurst *et al.* 2006; Ehrlich and Mirmoradi 2013) concluding that much higher displacement measured at the face of the wrapped wall than the segmental block wall. It indicates that the rigidity of wall face is an important parameter, which is comparable to the parametric study results that the shear stiffness between segment blocks (k_{sbb}) presents significant effect on the wall face deformation. The coefficient of variance in the unit weight of soil is within the range of 3% ~ 7% (Duncan *et al.* 2000). Compared with the other parameters, this magnitude of variance is much smaller (Walters *et al.* 2002; Huang and Bathurst 2009). Therefore, it is not included into the numerical experiments, though the unit weight of soil has strong effect on the maximum wall deformation. The effect of wall geometry parameters including wall height (H) and facing batter (ω) are also studied. As anticipated, the principals of slope stability apply here that the wall face deformation is significantly increased with an increasing wall height and a steeper wall inclination (*i.e.*, a smaller facing batter). Allen *et al.* (2003) defined a global index reinforcement stiffness value as the secant tensile stiffness (J) of an individual reinforcement layer divided by the vertical spacing (S) between reinforcement layers. This index is important to geosynthetic reinforced retaining wall for it can quantitatively express the extent of reinforcement. The numerical analysis performed in this study (Fig. 1) indicate that a larger global stiffness induce less wall face displacement. It is comparable to the experiment results reported in Bathurst *et al.* (2010) and the numerical analysis of Rowe and Ho (1998).

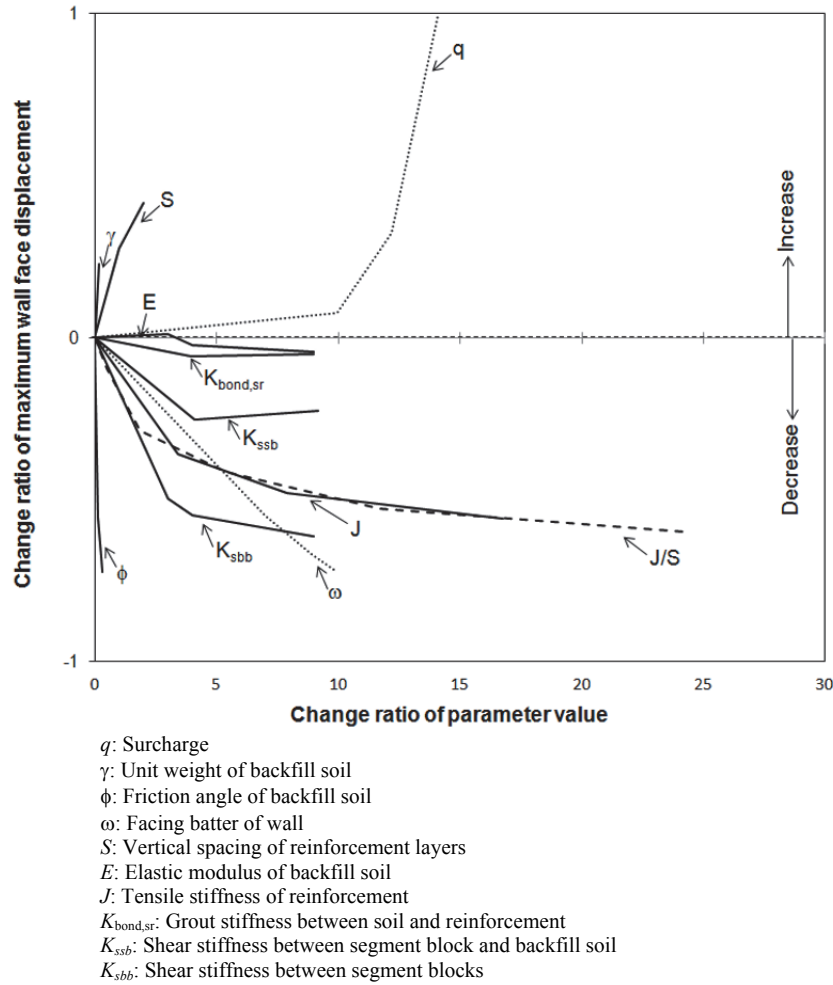


Fig. 1 Parametric analysis of important factors on the wall face deformation

In summary, the following six parameters: friction angle of backfill soil (ϕ_s), shear stiffness between segment blocks (k_{sbb}), wall height (H), facing better (ω), global index reinforcement stiffness value (J/S), along with surcharge loading on retaining wall (q), are selected to be variables in the numerical experiments. It is noted that the compaction energy is not considered though it is important on affecting the magnitude of maximum deformation during construction (Bathurst *et al.* 2010) because this study is more interested on the deformation after construction. The parameter values applied in the experiments are listed in Table 1. In total,

an experiment set consisting of 729 simulations by varying design parameters is conducted. The combination of parameter values covers a wide range of material properties, geometry, and surcharge condition, could be encountered in a geosynthetic reinforced segment retaining wall.

3. APPROXIMATED EQUATION FOR MAXIMUM FACE DEFORMATION OF SEGMENT MSE WALL

A database containing maximum wall face deformation (dependent) corresponding to different combinations of design parameters is generated after conducting the numerical experiment. An approximated equation is derived by regressing the dependent and design parameters in the database. The dependent is expressed in a dimensionless form as (δ_{max}/H) by normalizing the maximum wall face deformation (δ_{max}) by the height of retaining wall (H). The design parameters include dimensional factors of H , ω , J , S and $\tan(\phi)$, and dimensionless factors such as $x_1 = q/(\gamma H)$, $x_2 = \ln(\gamma HS/J)$, $x_3 = \ln(\gamma/K_{sbb})$, $x_4 = H/S$, $x_5 = S/(H \tan(\phi))$, $x_6 = 1 - \tan(\omega)$. Table 1 lists the values for these dimensionless parameters. The range in the dimensionless parameters is large. It should accommodate most practical construction of segment mechanically stabilized earth walls for estimating wall face deformation with this equation.

Table 1 Parameter values used in numerical experiments

Parameter	Parameter value
Friction angle of backfill soil, ϕ_s ($^\circ$)	35, 40, 45
Cohesion of backfill soil (kPa)	0.01
Elastic modulus of backfill soil, E_s (MPa)	40
Elastic modulus of segment (MPa)	400
Ultimate tensile strength of reinforcement (kN/m)	100
Shear stiffness between segment blocks, K_{sbb} (MPa/m)	10, 50, 100
Shear stiffness between segment block and backfill soil, K_{ssb} (MPa/m)	5
grout stiffness between soil and reinforcement, $K_{bond,sr}$ (MPa)	5
Tensile stiffness of reinforcement, J/S (kPa)	833, 1666, 3333
Wall height, H (m)	4, 6, 8
Facing batter, ω ($^\circ$)	0, 5, 10
Surcharge, q (kPa)	0, 10, 20
Unit weight of backfill soil, γ_s (kN/m ³)	16.8

The equation is regressed in the pattern as

$$\{C\} = [A] \cdot \{B\} \tag{1}$$

where $\{C\}$ is the dimensionless independent matrix $\ln(\delta_{max}/H)_i$, while $[A]$ is the independent parameter matrix and $\{B\}$ is the regression coefficient corresponding to independent parameters $[A]$. As learned from the parametric analysis results that the wall face deformation of a geosynthetic reinforced segment retaining wall is a nonlinear response to design parameters. Response surface methodology (RSM) is a collection of statistical and mathematical techniques useful for developing, improving, and optimizing processes. The RSM approach is used to develop a suitable second order equation for describing the relationship. For the detail of applying RSM in regressing the database please refer to Lin *et al.* (2016).

The approximated equation based on the 729 numerical simulation results is proposed in Eq. (2) as follows:

$$\begin{aligned}
 y = & \beta_0 + \beta_1 x_1 + \beta_2 x_2 + \beta_3 x_3 + \beta_4 x_4 + \beta_5 x_5 + \beta_6 x_6 \\
 & + \beta_7 x_1^2 + \beta_8 x_2^2 + \beta_9 x_3^2 + \beta_{10} x_4^2 + \beta_{11} x_5^2 + \beta_{12} x_6^2 \\
 & + \beta_{13} x_1 x_2 + \beta_{14} x_1 x_3 + \beta_{15} x_1 x_4 + \beta_{16} x_1 x_5 + \beta_{17} x_1 x_6 \\
 & + \beta_{18} x_2 x_3 + \beta_{19} x_2 x_4 + \beta_{20} x_2 x_5 + \beta_{21} x_2 x_6 \\
 & + \beta_{22} x_3 x_4 + \beta_{23} x_3 x_5 + \beta_{24} x_3 x_6 \\
 & + \beta_{25} x_4 x_5 + \beta_{26} x_4 x_6 \\
 & + \beta_{27} x_5 x_6 + \epsilon_1 + \epsilon_2
 \end{aligned} \tag{2}$$

The regression results including each dependent term (x_i) and its corresponding coefficient (β_i) are listed in Table 2. Different

Table 2 Coefficient values for response surface equation

No.	Coefficient	Value
1	β_0	- 1.3050
2	β_1	- 2.4671
3	β_2	- 0.5170
4	β_3	1.8156
5	β_4	0.2729
6	β_5	1.6811
7	β_6	- 4.9994
8	β_7	5.8184
9	β_8	0.0883
10	β_9	0.0388
11	β_{10}	- 0.0074
12	β_{11}	- 4.9496
13	β_{12}	2.5372
14	β_{13}	0.0716
15	β_{14}	- 0.1312
16	β_{15}	0.1570
17	β_{16}	2.5218
18	β_{17}	- 0.1443
19	β_{18}	- 0.0153
20	β_{19}	0.0502
21	β_{20}	1.9965
22	β_{21}	0.7818
23	β_{22}	- 0.0234
24	β_{23}	- 0.8039
25	β_{24}	- 0.8657
26	β_{25}	1.6443
27	β_{26}	- 0.1146
28	β_{27}	0.5978

forms of $[A]$ has been tested for the best regression results. The analyses' results reveal that $[A]$ which is composed of these terms fits best. It is noted that two model uncertainties are included into the approximated equations. The first model uncertainty, ϵ_1 , refers to the variance between numerical simulation result and actual face deformation measurement. The second model uncertainty, ϵ_2 , refers to the variance between approximated equation prediction and numerical simulation result.

4. PROBABILISTIC CHARACTERISTICS OF MAXIMUM FACE DEFORMATION OF SEGMENT MSE WALL

The uncertainties in the calculated wall face deformation from the approximated equation include the parameter uncertainties and model uncertainties (ϵ_1 and ϵ_2). To estimate the magnitude of the model uncertainty ϵ_1 , the measured maximum wall deformation of model walls #1, #2, and #3 at the end of construction and under the application of surcharge loading reported in Hatami and Bathurst (2005, 2006), denoted as $(\delta_{max})_{Test}$, and the numerical simulated maximum wall deformation from the FLAC codes developed in this study, denoted as $(\delta_{max})_{FLAC}$, are compared. The probability density function of model uncertainty ϵ_1 is assumed to follow Gaussian distribution with a mean value and a standard deviation, *i.e.*, it is shown as $N(\mu_1, \sigma_1^2)$. Since the wall height is 3.6 m in Hatami and Bathurst (2005, 2006), μ_1 and σ_1 are calculated by Eq. (3). The data for estimating model uncertainty ϵ_1 is shown in Table 3. The calibration between measured data and numerical analysis results shows the model uncertainty ϵ_1 is about $N(-0.0012, 0.3422^2)$.

Table 3 Data applied in to Eq. (4) for estimating model uncertainty ϵ_1

Wall	$(\delta_{max})_{Test}$ (mm)	$(\delta_{max})_{FLAC}$ (mm)	$\ln\left(\frac{\delta_{max}}{3600}\right)_{Test} - \ln\left(\frac{\delta_{max}}{3600}\right)_{FLAC}$
1	2.73728	1.24066	0.791321
	1.91701	2.48132	- 0.25802
	3.80321	4.34978	- 0.13428
	5.20959	5.21674	- 0.00137
	5.53996	6.23318	- 0.1179
2	5.5703	6.53214	- 0.15929
	1.19776	1.30045	- 0.08226
	5.69911	2.70553	0.745012
	3.56448	4.63378	- 0.26235
	4.62893	6.75635	- 0.37816
	6.45327	7.23468	- 0.1143
3	7.61713	5.85949	0.262337
	2.096	2.2272	- 0.06071
	2.53161	3.64723	- 0.36511
	5.58505	6.39761	- 0.13583
	6.69214	7.04036	- 0.05073
		std	0.3422
		mean	0.0012

$$\mu_1 = \text{mean} \left[\ln \left(\frac{\delta_{\max}}{3600} \right)_{\text{Test}} - \ln \left(\frac{\delta_{\max}}{3600} \right)_{\text{FLAC}} \right] \quad (3a)$$

$$\sigma_1 = \text{std} \left[\ln \left(\frac{\delta_{\max}}{3600} \right)_{\text{Test}} - \ln \left(\frac{\delta_{\max}}{3600} \right)_{\text{FLAC}} \right] \quad (3b)$$

It is noted that the unit of δ_{\max} is in millimeters. The comparison of approximated equation prediction ($(\delta_{\max}/H)_{\text{Equation}}$) and numerical simulation result ($(\delta_{\max}/H)_{\text{FLAC}}$) is shown in Fig. 2, which shows a well agreement. To quantify the variance between approximated equation prediction and numerical simulation results, refer to the second model uncertainty, ε_2 , the probability density function is assumed to follow Gaussian distribution with a mean value and a standard deviation. It is shown as $N(\mu_2, \sigma_2^2)$. The mean value and standard deviation in model uncertainty ε_2 is estimated by using the following equation:

$$\mu_2 = \text{mean} \left[\ln \left(\frac{\delta_{\max}}{3600} \right)_{\text{FLAC}} - \ln \left(\frac{\delta_{\max}}{3600} \right)_{\text{Equation}} \right] \quad (4a)$$

$$\sigma_2 = \text{std} \left[\ln \left(\frac{\delta_{\max}}{3600} \right)_{\text{FLAC}} - \ln \left(\frac{\delta_{\max}}{3600} \right)_{\text{Equation}} \right] \quad (4b)$$

The model uncertainty ε_2 is calculated as $N(0, 0.0002^2)$. It indicates that the approximated equation models the maximum wall face deformation well with little bias. This value is marginal enough to be ignored in practical engineering. To accommodate with the two sources of model uncertainties in the approximated equation (Eq. (2)), it is identified as a normal distribution of mean bias of -0.0012 and a standard deviation of about 0.3422 , which is equal to the square root of the summation of variances of two sources of uncertainties, ε_1 and ε_2 .

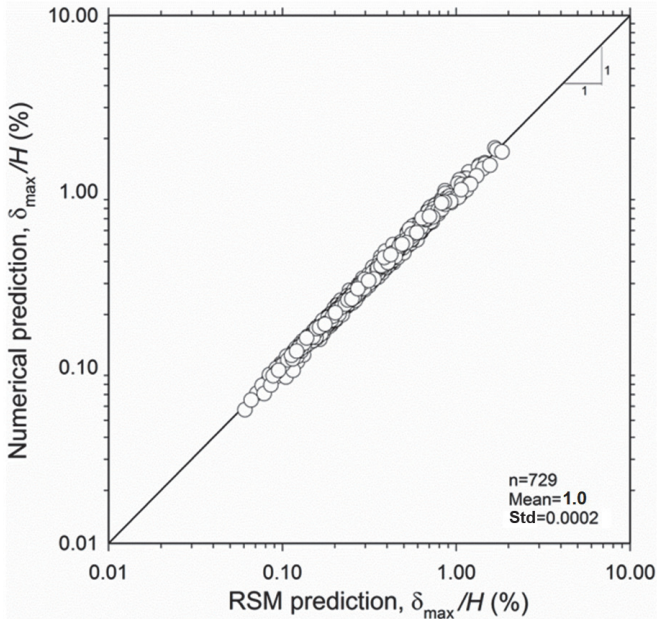


Fig. 2 Comparison between $(\delta_{\max}/H)_{\text{FLAC}}$ simulated from numerical program and $(\delta_{\max}/H)_{\text{Equation}}$ calculated from approximated equation

Table 4 Statistical properties of parameter for base case

Parameter	Distribution	Mean	COV
Backfill soil unit weight, γ_s (kN/m ³)	Lognormal	20	10%
Wall height, H (m)	Deterministic	4	0%
Facing batter, ω (degree)	Deterministic	5	0%
Soil friction angle, ϕ_s (degree)	Lognormal	40	10%
Reinforcement axial stiffness, J (kN/m)	Lognormal	1000	10%
Block-block interface shear stiffness, k_{sbb} (MPa/m)	Lognormal	50	10%
Surcharge pressure, q (kPa)	Lognormal	10	10%

Since the independent variables are random, there will likewise be uncertainty in the dependent variable (*i.e.*, the normalized maximum wall face deformation). The uncertainty in the approximated equation needs to be accounted for by considering the variability of parameters in it. The attributes and statistical properties of these parameters are listed in Table 4. The attribute of each parameter refers to natural characteristics and previous studies (Haldar and Tang 1979; Popescu 1995; Lacasse and Nadim 1996; Popescu 1996; Popescu 1997; Fenton 1999). These variables which exist in the approximated equation are treated as random variables in the subsequent study under probabilistic framework.

A series of Monte Carlo simulations are conducted by varying parameters values from the base case. Note that the Monte Carlo simulation with multiple realizations can be manipulated easily because the approximate equation has a simple form which can be calculated with spreadsheet or by computer program. The histogram of maximum of 1,000 simulations of wall face deformation of the base case is shown in Fig. 3, along with a fitted probability density function (PDF) of lognormal distribution. The lognormal PDF fits the histogram of raw data well, which indicates that the maximum wall face deformation is approximately log-normally distributed. The characteristic parameters (shape and scale parameters) λ and ζ for this lognormal distribution can be calculated by the following equations where i is the index of summation and n is the number of realizations:

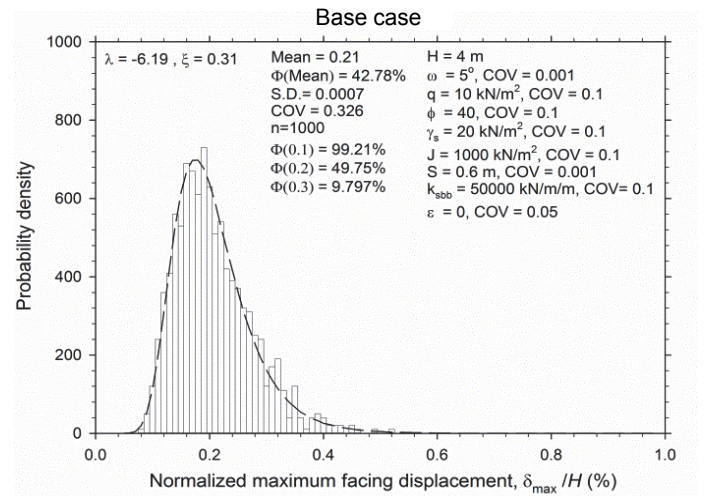


Fig. 3 Histogram of simulated maximum wall face deformation for base case

$$\lambda = \frac{1}{n} \sum_{i=1}^n \left(\frac{\delta_{\max}}{H} \right)_i \quad (5a)$$

$$\zeta = \sqrt{\frac{\sum_{i=1}^n \left[\left(\frac{\delta_{\max}}{H} \right)_i - \lambda \right]^2}{n-1}} \quad (5b)$$

For this base case, λ and ζ are -6.19 and 0.31 , respectively. This information is valuable for estimating the probability which fails to satisfy the prerequisite performance condition of segment MSE wall. The target maximum wall faces a deformation ratio (δ_{\max}/H) which can be set according to the importance and the utility of the reinforced soil structure. The probability that exceeds this prerequisite performance condition $\delta_{\max}/H_{\text{assume target}}$ can be calculated from the following lognormal probability distribution by using statistical tool (for example, LOGNORM.DIST() in EXCEL). For example, for the base case, if the allowed prerequisite performance condition is set as 0.2% of δ_{\max}/H , the exceedance probability would be calculated as 49.75% (i.e., $P_f(\delta_{\max}/H < 0.2\%) = 49.75\%$). For simplicity, the exceedance probability is denoted as $\Phi(x)$ where x is the designed normalized face displacement. That is, $P_f(\delta_{\max}/H < 0.2\%)$ is denoted as $\Phi(0.2)$. The failure probabilities (P_f) corresponding to the tolerable wall face deformation ratio of 0.1% of δ_{\max}/H is 99.21% (i.e., $\Phi(0.1) = 99.21\%$). It indicates the failure probability increases with stricter wall face deformation criterion. Similarly, for a looser wall face deformation criterion, for example, $0.3(\delta_{\max}/H)$, the exceedance probability ($\Phi(0.3)$) is 9.797%.

It is of interest to investigate the relative significance of different design parameters over the probabilistic characteristics of maximum wall face deformation. To achieve the parametric analysis, the process of conducting 1000 realizations of the Monte Carlo Simulation is similarly performed for 14 cases. In each case, one parameter is changed from the value of base case. These cases are believed to be sufficient to demonstrate the main features of the influence of important parameters on reinforced segment wall face deformation. For each case, the obtained histogram can be well fitted with the lognormal distribution function and they are statistically analyzed to calculate the shape and scale parameters for best fit lognormal distribution, as shown in Fig. 4. The excess probabilities for different prerequisite maximum wall face deformation ratio (0.1%, 0.2%, and 0.3% δ_{\max}/H) are calculated. The parametric analysis results are tabulated in Table 5.

Analysis results of varying parameter values on the excess probability are shown in Fig. 5. The sensitivity of these parameters on probability is examined. The nearly horizontal curve for all deformation criterion plotted in Fig. 5(a) indicate that the soil unit weight (γ_s) owns marginal effect on the failure probability as it ranges between 16.8 and 20 kN/m³. Figure 5(b) shows the effect of friction angle of backfill soil (ϕ_s) on failure probability. It can be seen that failure probability increases significantly with an increase in (ϕ_s), which implied the dominant influence of friction angle of backfill soil of reinforced retaining wall. The (ϕ_s) is sensitive because the wall is composed of backfill soil.

For a soil of larger friction angle, its stability is greater and it can sustain more loading at the same strain level. It demonstrates the importance of compaction of backfill soil in controlling the deformation of reinforced retaining wall. The tensile stiffness of the reinforcement is normalized by the spacing between layers of reinforcement as the global index reinforcement stiffness value (J/S). As shown in Fig. 5(c), the failure probability for maximum wall face deformation criterion decreases significantly as (J/S) increases. For the wall which is reinforced by stiffer material or is placed by more layers of reinforcement, it is more resistant to the occurrence of lateral deformation. A noticeable trend is found that the failure probability decreases with an increase in shear stiffness between segment blocks (k_{sbb}), as shown in Fig. 5(d). The shear stiffness between segment blocks (k_{sbb}) controls the face deformability of a segment reinforced wall. A larger magnitude of (k_{sbb}) implies the wall face is more difficult to deform laterally. The influence of geometry parameters of retaining wall on its face deformation is shown in Figs. 5(e) and 5(f). As expected from the geotechnical engineering that the stability of a retaining wall reduces for a higher and steeper wall, the probability exceeding certain performance criterion increases as the wall height (H) increases and the facing batter (ω) is steeper. The effect of surcharge (q) acting on the wall top is shown in Fig. 5(g). It shows that at any performance criterion, there is a significant increase of failure probability with an increase in surcharge magnitude. It is attributed to an increase of earth pressure within retaining wall induced by the application of surcharge. In general, the geotechnical principals apply to factor of safety also apply to deformation characteristics of a segment MSE wall.

The effect of variance of design parameters on wall face deformation is also studied and presented in Figs. 6(a) to 6(e). They are shown in dash lines and the nearly horizontal trend indicate that the variance in design parameter on exceedance probability of certain wall face deformation criterion is marginal, compared with the mean value in the design parameters. The analysis results show that failure probability is insignificantly changed as coefficient of variation in parameters varies significantly (5% to 20% for q , for a fixed value of design parameter. In general, failure probability increases slightly with an increase in the variance in parameters. This phenomenon can be explained by the distribution tail. An increase in the variance in parameters and in models would generate more extreme cases during simulation thus increase the frequency of extreme cases in the right tail of probabilistic distribution. Because the estimation of failure probability is to integrate the cases which exceed the specified criteria of wall face deformation ratio, a fatter tail distribution produces a larger failure probability. Figure 6(f) shows the effect of model uncertainty. Observed from this figure, it is clearly found that the failure probability is significantly increased as the coefficient of variation in the approximated equation (cov_M) increases from 0.2 to 0.6. It indicates that the failure probability is sensitive to the magnitude of total model uncertainty. This analysis highlights that, relative to the uncertainty in design parameters, the model uncertainty is much more crucial. The development of approximated equation with high quality of low magnitude of model uncertainty is important to conduct probability analysis of segment reinforced wall face deformation.

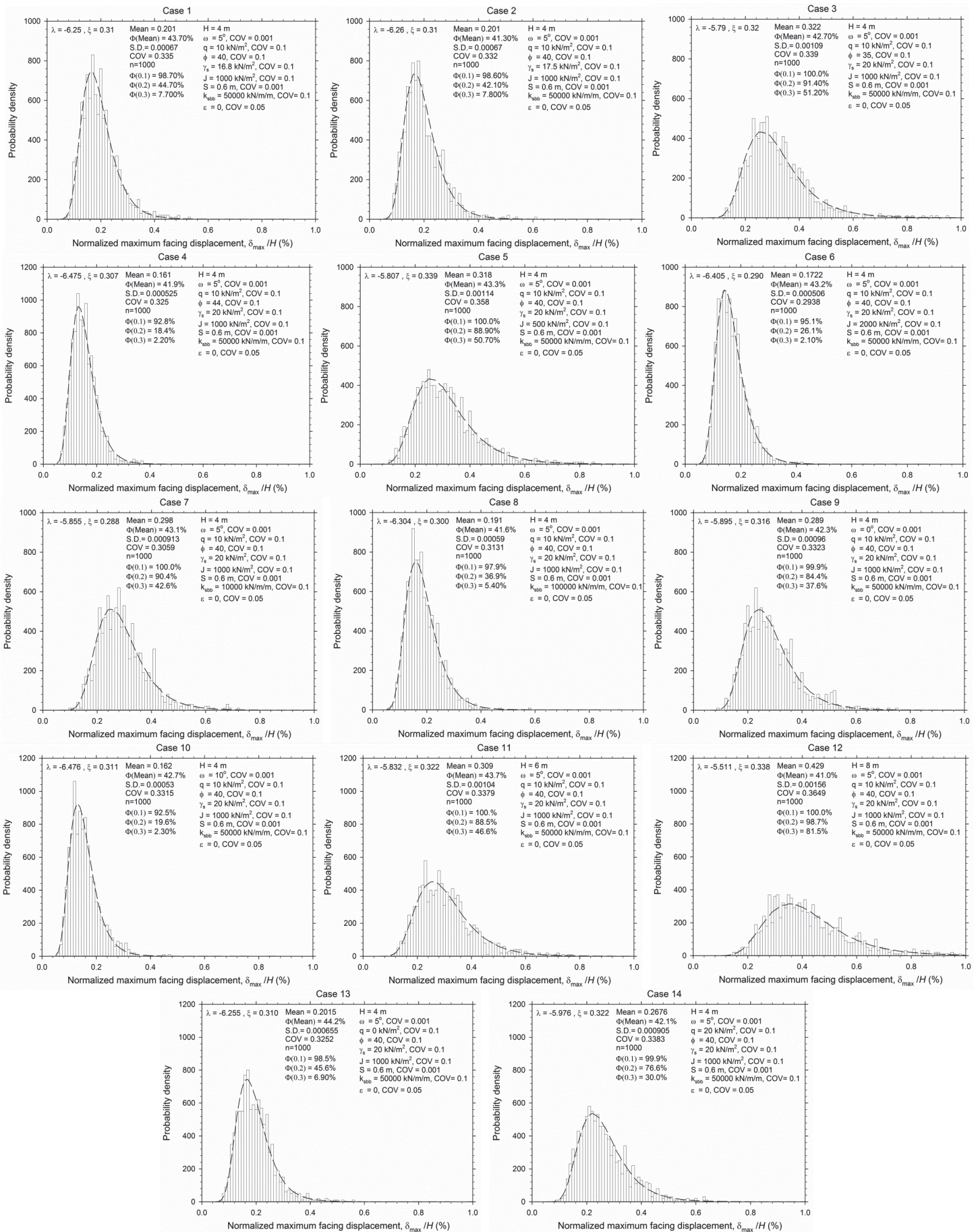


Fig. 4 Histograms of simulated maximum wall face deformations for case 1 to case 14

Table 5 Parametric analysis results of best fit lognormal distribution characteristics and excess probabilities for different wall face deformation ratios

Case	Variable changed	λ	ζ	Probability of failure		
				$\left(\frac{\delta_{max}}{H}\right) = 0.1\%$	$\left(\frac{\delta_{max}}{H}\right) = 0.2\%$	$\left(\frac{\delta_{max}}{H}\right) = 0.3\%$
Base-case	-	-6.19	0.31	99.21%	49.75%	9.797%
1	$\gamma = 16.8$	-6.25	0.31	98.70%	44.70%	7.700%
2	$\gamma = 17.5$	-6.26	0.31	98.60%	42.10%	7.800%
3	$\phi = 35$	-5.79	0.32	100.00%	91.40%	51.20%
4	$\phi = 44$	-6.48	0.31	92.80%	18.40%	2.200%
5	$J = 500$	-5.81	0.34	100.00%	88.90%	50.70%
6	$J = 2000$	-6.41	0.29	95.10%	26.10%	2.100%
7	$K_{sbb} = 10000$	-5.86	0.29	100.00%	90.40%	42.60%
8	$K_{sbb} = 100000$	-6.30	0.30	97.90%	36.90%	5.400%
9	$\omega = 0$	-5.90	0.32	99.90%	84.40%	37.60%
10	$\omega = 10$	-6.48	0.31	92.50%	19.60%	2.300%
11	$H = 6$	-5.83	0.32	100.00%	88.50%	46.60%
12	$H = 8$	-5.51	0.34	100.00%	98.70%	81.50%
13	$q = 0$	-6.26	0.31	98.50%	45.60%	6.900%
14	$q = 20$	-5.98	0.32	99.90%	76.60%	30.00%

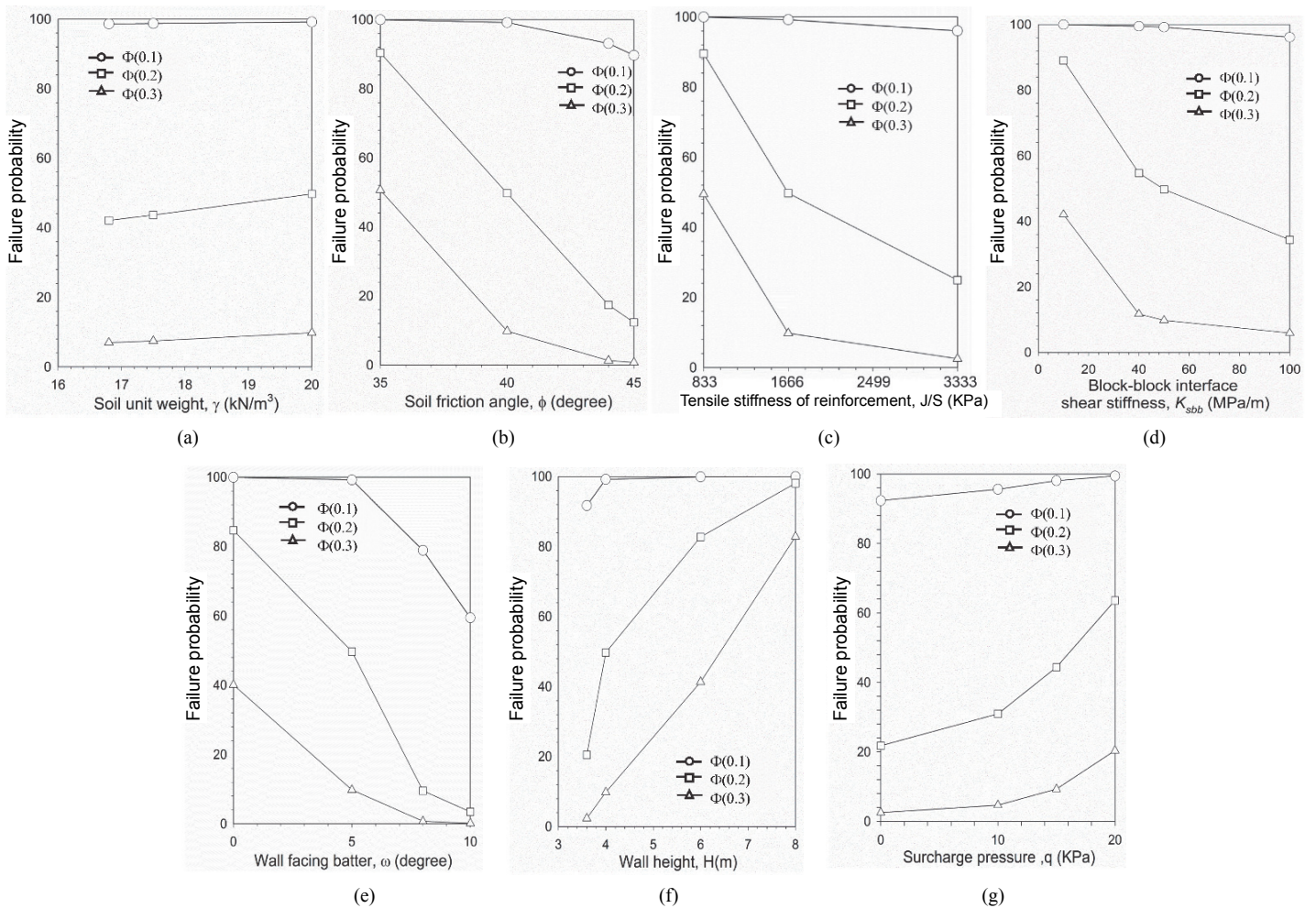


Fig. 5 Effect of parameter value on the exceedance probability of maximum wall face deformation

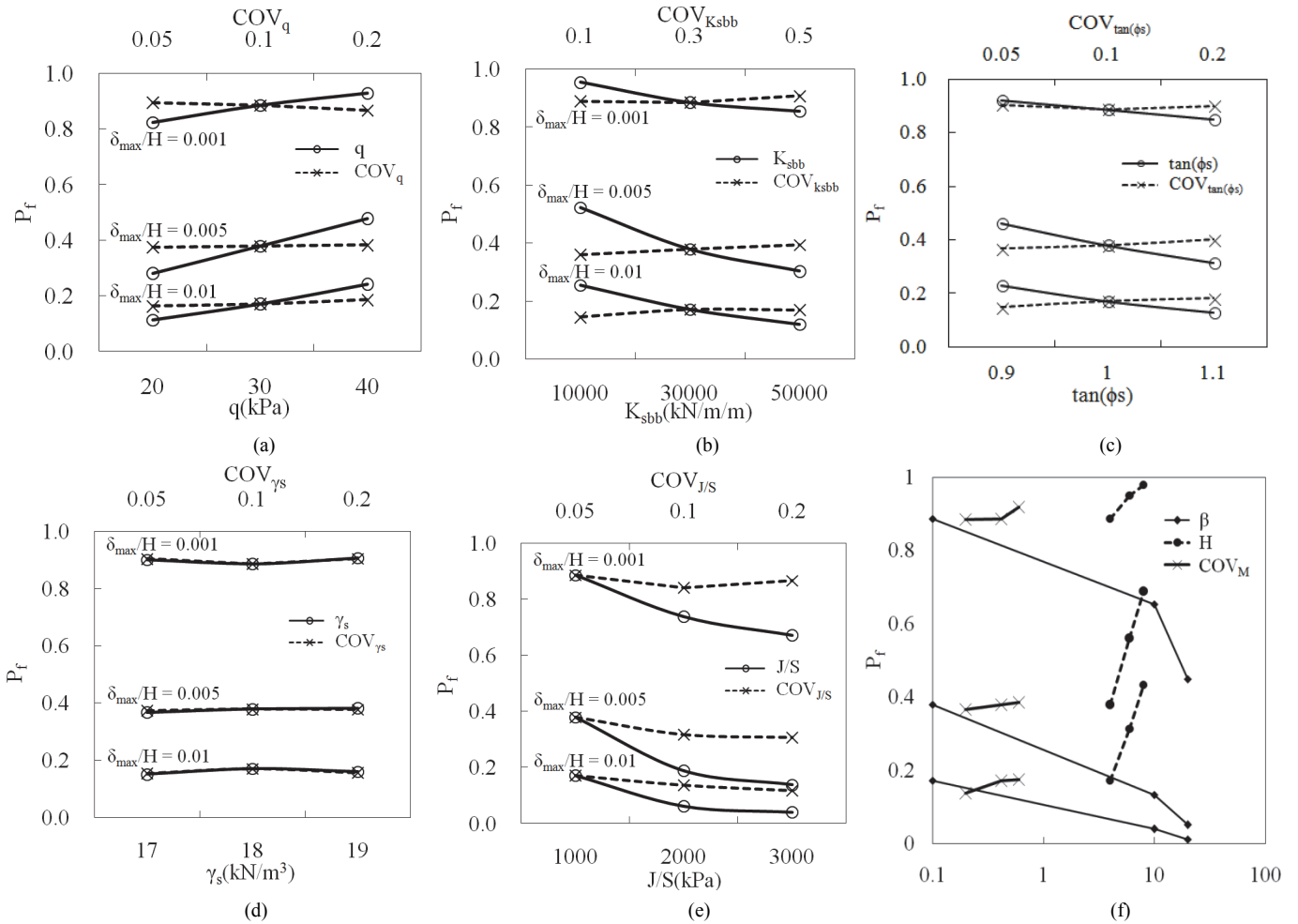


Fig. 6 Effect of variance in parameters on the exceedance probability of maximum wall face deformation

5. CONCLUSIONS

The application of geosynthetics to reinforce geotechnical structures progressively improves the material manufacture, design method, and construction. The design and analysis of geosynthetic reinforced retaining walls are mostly based on deterministic value of material properties. However, the recent trend is to conduct probabilistic design and analysis. Meanwhile, the consideration on performance of constructed facilities has increased in parallel with the advent of technology. This is even true for deformation behavior of reinforced segment retaining wall which is sensitive to the soil properties, segment stiffness, and geosynthetic stiffness of significant variation.

The study presented here exemplifies how the probabilistic analysis of serviceability criteria may be achieved in geosynthetic reinforced segment walls. Especially, the maximum wall face deformation is of interest because it is index to serviceability. In this study, a numerical model for simulating lateral deformation of geosynthetic reinforced segment wall is developed. A set of numerical experiment is conducted to generate a database of maximum wall face displacement as different combination of design parameters. An approximated equation of normalized maximum wall face displacement for the reinforced segment retaining walls as functions of design parameters is regressed from the database. With the application of Monte Carlo Simulation technique on the

approximated equation, the probabilistic distribution of normalized maximum wall face displacement is available. It can be well fitted as a lognormal distribution. The exceedance probability of geosynthetic reinforced segment wall under defined serviceability criterion can be estimated from the histogram. Moreover, the reliability based design of geosynthetic reinforced segment wall on the criterion of maximum wall face deformation is also feasible using the methodology presented here.

This approximated equation is an easy and accurate tool to estimate the probabilistic characteristic of a geosynthetic reinforced segment wall. It is noted that some factors such as compaction process, earthquake, rainfall and drainage, and foundation instability will induce additional wall face deformation. The scope of this study is limited to estimate the deformation of segment MSE wall after construction is completed and without other potential adverse factors. In general, the geotechnical principals apply to factor of safety also apply to deformation characteristics of a segment MSE wall. The probability of exceeding the deformation tolerance increases with an increase in wall height, and applied surcharge and with a steeper facing batter. The enhancement of material properties, such as larger friction angle of backfill soil, a stiffer reinforced material or a narrower spacing of reinforced material placement, along with an increase in shear stiffness between segment blocks, can significantly improve the performance in terms of wall face deformation. In general, failure probability

increases slightly with an increase in the variance in parameters. Compared with the mean value in the design parameters, the variance in design parameter on exceedance probability of certain wall face deformation criterion is marginal. However, the model uncertainty in the developed approximated equation is much more crucial. The successful implementation of this approach is on the premise of developing a sound and simple approximated equation. The inclusion of more measurement data of model walls or field walls will calibrate the numerical model and thus after the approximated equation to a better extent.

FUNDING

The authors received no funding for this work.

DATA AVAILABILITY

The data and/or computer codes used/generated in this study are available from the corresponding author on reasonable request.

NOTATIONS

The following symbols are used in this paper:

$[A]$	The independent parameter matrix
$\{B\}$	The regression coefficient
$\{C\}$	The dimensionless independent matrix
cov	Coefficient of variation
E_s	Elastic modulus of backfill soil [MPa]
H	Wall height [m]
i	Index of summation
J	Secant tensile stiffness of reinforcement [kN/m]
$k_{bond, sr}$	grout stiffness between soil and reinforcement [MPa]
K_{sbb}	Shear stiffness between segment blocks [MPa/m]
K_{ssb}	Shear stiffness between segment block and backfill soil [MPa/m]
M	Model uncertainty
n	Number of realizations
P_f	Failure probabilities
q	Surcharge [kPa]
S	Vertical spacing between reinforcement layers [m]
$S.D.$	Standard deviation of simulated maximum wall face deformation [mm]
δ_{max}	The maximum wall face deformation [mm]
ε	Model uncertainty in approximated equation
ε_1	Model uncertainty of Test and FLAC
ε_2	Model uncertainty of FLAC and Equation
ϕ, ϕ_s	Friction angle of backfill soil [°]
Φ	Exceedance probability of designed face displacement
γ, γ_s	Backfill soil unit weight [kN/m ³]
λ	Shape parameters
μ_1	Mean value of Test and FLAC
μ_2	Mean value of FLAC and Equation
σ_1	Standard deviation of Test and FLAC
σ_2	Standard deviation of FLAC and Equation
ω	Facing batter [°]
ζ	Scale parameters

REFERENCES

- Allen, T.M., Bathurst, R.J., and Berg, R.R. (2002). "Global level of safety and performance of geosynthetic walls: a historical perspective." *Geosynthetics International*, **9**(5-6), 395-450. <https://doi.org/10.1680/gein.9.0224>
- Allen, T.M., Bathurst, R.J., Holtz, R.D., Walters, D., and Lee, W.F. (2003). "A new working stress method for prediction of reinforcement loads in geosynthetic walls." *Canadian Geotechnical Journal*, **40**(4), 976-994. <https://doi.org/10.1139/t03-051>
- Basheer, I.A. and Najjar, Y.M. (1994). "Reliability based design of reinforced earth retaining walls." *Transportation Research Record*, **1526**, 64-78. <https://doi.org/10.1177/0361198196152600109>
- Basma, A.A., Barakat, S.A., and Omar, M.T. (2003). "Reliability based risk index for the design of reinforced earth structures." *Geotechnical and Geological Engineering*, **21**, 225-242. <https://doi.org/10.1023/A:1024932408001>
- Bathurst, R.J., Allen, T.M., and Walters, D.L. (2002). "Short-term strain and deformation behavior of geosynthetic walls at working stress conditions." *Geosynthetics International*, **9**(5-6), 451-482. <https://doi.org/10.1680/gein.9.0225>
- Bathurst, R.J., Allen, T.M., and Walters, D.L. (2005). "Reinforcement loads in geosynthetic walls and the case for a new working stress design method." *Geotextiles and Geomembranes*, **23**(4), 287-322. <https://doi.org/10.1016/j.geotextmem.2005.01.002>
- Bathurst, R.J., Miyata, Y., and Allen, T.M. (2010). "Facing displacements in geosynthetic reinforced soil walls. Invited keynote paper." *Proceedings of Earth Retention Conference 3 (ER2010)*, ASCE Geo-Institute, Bellevue, Washington, 442-459. [https://doi.org/10.1061/41128\(384\)45](https://doi.org/10.1061/41128(384)45)
- Bathurst, R.J., Nernheim, A., Walters, D.L., Allen, T.M., Burgess, P., and Saunders, D.D. (2009). "Influence of reinforcement stiffness and compaction on the performance of four geosynthetic-reinforced soil walls." *Geosynthetic International*, **16**(1), 43-59. <https://doi.org/10.1680/gein.2009.16.1.43>
- Bathurst, R.J., Vlachopoulos, N., Walters, D.L., Burgess, P.G., and Allen, T.M. (2006). "The influence of facing stiffness on the performance of two geosynthetic reinforced soil retaining walls." *Canadian Geotechnical Journal*, **43**(12), 1225-1237. <https://doi.org/10.1139/t06-076>
- Chalermyanont, T. and Benson, C. (2004). "Reliability-based design for internal stability of mechanically stabilized earth (MSE) walls." *Journal of Geotechnical and Geoenvironmental Engineering*, ASCE, **130**(2), 163-173. [https://doi.org/10.1061/\(ASCE\)1090-0241\(2004\)130:2\(163\)](https://doi.org/10.1061/(ASCE)1090-0241(2004)130:2(163))
- Chalermyanont, T. and Benson, C. (2005a). "Reliability-based design for external stability of mechanically stabilized earth (MSE) walls." *International Journal of Geomechanics*, ASCE, **5**(3), 196-205. [https://doi.org/10.1061/\(ASCE\)1532-3641\(2005\)5:3\(196\)](https://doi.org/10.1061/(ASCE)1532-3641(2005)5:3(196))
- Chalermyanont, T. and Benson, C. (2005b). "Method to estimate the system probability of failure of mechanically stabilized earth (MSE) walls." GSP 140 slopes and retaining structures under seismic and static conditions, *Proceedings of Sessions of the Geo-Frontiers 2005 Congress*.
- Duncan, J.M. (2000). "Factors of Safety and Reliability in Geotechnical Engineering." *Journal of Geotechnical and Geoenvironmental Engineering*, ASCE, **126**(3), 307-316. [https://doi.org/10.1061/\(ASCE\)1090-0241\(2000\)126:4\(307\)](https://doi.org/10.1061/(ASCE)1090-0241(2000)126:4(307))
- Duijnen, P.G. van, Linthof, T., Brok, C.A.J.M., and Eekelen, S.J.M. van. (2014). "Measuring deformations of a 10 m high

- geosynthetic reinforced earth retaining wall." *Proceedings of 5th European Geosynthetics Congress*, Valencia, Spain.
- Ehrlich, M. and Mirmoradi, S.H. (2013). "Evaluation of the effects of facing stiffness and toe resistance on the behavior of GRS walls." *Geotextiles and Geomembranes*, **40**(5), 28-36. <https://doi.org/10.1016/j.geotexmem.2013.07.012>
- Ehrlich, M., Mirmoradi, S.H., and Saramago, R.P. (2012). "Evaluation of the effects of compaction on the behavior of geosynthetic-reinforced soil walls." *Geotextiles and Geomembranes*, **34**(5), 108-115. <https://doi.org/10.1016/j.geotexmem.2012.05.005>
- Fenton, G.A. (1999). "Random field modeling of CPT data." *Journal of Geotechnical and Geoenvironmental Engineering*, ASCE, **125**(6), 486-498. [https://doi.org/10.1061/\(ASCE\)1090-0241\(1999\)125:6\(486\)](https://doi.org/10.1061/(ASCE)1090-0241(1999)125:6(486))
- Haldar, A.M. and Tang, W.H. (1979). "Probabilistic evaluation of liquefaction potential." *Journal of the Geotechnical Engineering Division*, ASCE, **105**(2), 145-163.
- Hatami, K. and Bathurst, R.J. (2005). "Development and verification of a numerical model for the analysis of geosynthetic reinforced-soil segmental walls." *Canadian Geotechnical Journal*, **42**(4), 1066-1085. <https://doi.org/10.1139/t05-040>
- Hatami, K. and Bathurst, R.J. (2006). "Numerical model for reinforced soil segmental walls under surcharge loading." *Journal of Geotechnical and Geoenvironmental Engineering*, ASCE, **132**(6), 673-684. [https://doi.org/10.1061/\(ASCE\)1090-0241\(2006\)132:6\(673\)](https://doi.org/10.1061/(ASCE)1090-0241(2006)132:6(673))
- Hattamleh, O.A.I. and Muhunthan, B. (2006). "Numerical procedures for deformation calculations in the reinforced soil walls." *Geotextiles and Geomembranes*, **24**(1), 52-57. <https://doi.org/10.1016/j.geotexmem.2005.07.001>
- Hirakawa, D., Takaoka, H., Tatsuoka, F., and Uchimura, T. (2004). "Deformation characteristics of geosynthetics retaining wall loaded on the crest." *Proceedings of Asian regional Conference on Geosynthetics*, 240-247.
- Huang, B. and Bathurst, R.J. (2009). "Evaluation of soil-geogrid pullout models using a statistical approach." *Geotechnical Testing Journal*, **32**(6), 102460. <https://doi.org/10.1520/GTJ102460>
- Itasca Consulting Group, Inc. (2001). *Fast Lagrangian Analysis of Continua*, Version 4.0, Volume I, II, III, IV.
- Lacasse, S. and Nadim, F. (1996). "Uncertainties in characterizing soil properties." *Proceedings of ASCE GED Spec. Conference on Uncertainty in the Geologic Environment: From Theory to Practice*, Madison, Wisconsin, 49-75.
- Karpurapu, R. and Bathurst, R.J. (1995). "Behaviour of geosynthetic reinforced soil retaining walls using the finite element method." *Computers and Geotechnics*, **17**(3), 279-299. [https://doi.org/10.1016/0266-352X\(95\)99214-C](https://doi.org/10.1016/0266-352X(95)99214-C)
- Kibria, G., Hossain, S., and Khan, M.S. (2014). "Influence of soil reinforcement on horizontal displacement of MSE wall." *International Journal of Geomechanics*, ASCE, **14**(1), 130-141. [https://doi.org/10.1061/\(ASCE\)GM.1943-5622.0000297](https://doi.org/10.1061/(ASCE)GM.1943-5622.0000297)
- Lin, H.I., Cardany, C.P., Sun, L.X., and Hashimoto, H. (2000). "Finite element study of a geosynthetic-reinforced soil retaining wall with concrete-block facing." *Geosynthetics International*, **7**(2), 137-162. <https://doi.org/10.1680/gein.7.0170>
- Lin, B.H., Lin, B.H., Yu, Y., Bathurst, R.J., and Liu, C.N. (2016). "Deterministic and probabilistic prediction of facing deformations of geosynthetic-reinforced MSE walls using a response surface approach." *Geotextiles and Geomembranes*, **44**, 813-823. <https://doi.org/10.1016/j.geotexmem.2016.06.013>
- Liu, H., Wang, X., and Song, E. (2009). "Long-term behavior of GRS retaining walls with marginal backfill soils." *Geotextiles and Geomembranes*, **27**(4), 295-307. <https://doi.org/10.1016/j.geotexmem.2009.01.002>
- Onodera, S., Fukuda, N., and Nakane, A. (2004). "Long-term behaviour of geogrid reinforced soil walls." *Proceedings of 3rd GeoAsia*, Seoul, South Korea.
- Phoon, K.K. and Kulhawy, F.H. (1999). "Evaluation of geotechnical property variability." *Canadian Geotechnical Journal*, **36**(4), 625-639. <https://doi.org/10.1139/cgj-36-4-625>
- Popescu, R. (1995). *Stochastic Variability of Soil Properties: Data Analysis, Digital Simulation, Effects on System Behavior*. Ph.D. Dissertation, Princeton University, Princeton, NJ.
- Popescu, R., Prevost, J.H., and Deodatis, G. (1996). "Influence of spatial variability of soil properties on seismically induced soil liquefaction." *Uncertainty in the Geological Environment: From Theory to Practice*, Madison, Wisconsin, 1098-1112.
- Popescu, R., Prevost, J.H., and Deodatis, G. (1997). "Effects of spatial variability on soil liquefaction: some design recommendations." *Géotechnique*, **47**(5), 1019-1036. <https://doi.org/10.1680/geot.1997.47.5.1019>
- Rowe, R.K. and Ho, S.K. (1998). "Horizontal deformation in reinforced soil walls." *Canadian Geotechnical Journal*, **35**(2), 312-327. <https://doi.org/10.1139/t97-062>
- Rowe, R.K. and Skinner, G.D. (2001). "Numerical analysis of geosynthetic reinforced retaining wall constructed on a layered soil foundation." *Geotextiles and Geomembranes*, **19**(7), 387-412. [https://doi.org/10.1016/S0266-1144\(01\)00014-0](https://doi.org/10.1016/S0266-1144(01)00014-0)
- Ruiken, A., Ziegler, M., Vollmert, L., and Höhney, S. (2010). "Investigation of the compound behavior of geogrid reinforced soil." *Proceedings of 15th European Conference on Soil Mechanics and Geotechnical Engineering*, Athens, Greece.
- Sayed, S., Dodagoudar, G.R., and Rajagopal, K., (2008), "Reliability analysis of reinforced soil walls under static and seismic forces." *Geosynthetics International*, **15**(4), 246-257. <https://doi.org/10.1680/gein.2008.15.4.246>
- Suah, P.G. and Goodings, D.J. (2001). "Failure of geotextile-reinforced vertical soil walls with marginal backfill." *Transportation Research Report*, **1772**, 183-189. <https://doi.org/10.3141/1772-22>
- Turner, R. and Schweiger, H.F. (2000). "Reliability analysis for geotechnical problems via finite elements - a practical application." *Extended Abstracts International Conference on Geotechnical and Geological Engineering*, Australia, Melbourne, **11**, 1-6.
- Walters, D., Allen, T.M., and Bathurst, R.J. (2002). "Conversion of geosynthetic strain to load using reinforcement stiffness." *Geosynthetics International*, **9**(5-6), 483-523. <https://doi.org/10.1680/gein.9.0226>
- Yang, G., Liu, H., Lv, P., and Zhang, B. (2012). "Geogrid-reinforced lime-treated cohesive soil retaining wall: Case study and implications." *Geotextiles and Geomembranes*, **35**(6), 112-118. <https://doi.org/10.1016/j.geotexmem.2012.09.001>